Supplementary Information (SI) for ChemComm.
This journal is © The Royal Society of Chemistry 2026

Supplementary Information

Electronic Modulation and Interface Engineering via Amorphous Ceria for Enhanced OER in $NiMoO_4$ Heterostructures

Yudong Liu, Yani Hua and Zhan Gao*

School of Chemical Engineering and Technology, Xi'an Jiaotong University, No.28, Xianning West Road, Xi'an 710049, China

E-mail: zhangao18@xjtu.edu.cn

Materials and Methods

Materials

$Ni(NO_3)_2 \cdot 6H_2O$ was bought from Sinopharm Chemical Reagent Co. $(NH_4)_6Mo_7O_{24} \cdot 4H_2O$ and $Ce(NO_3)_3 \cdot 6H_2O$ were bought from Shanghai Aladdin Biochemical Technology Co., Ltd Nickel foam (NF) was bought from Kunshan Guangjiayuan Electronics.

Preparation of $NiMoO_4$

290.79 mg (1 mmol) of $Ni(NO_3)_2 \cdot 6H_2O$ and 182.14 mg of $(NH_4)_6Mo_7O_{24} \cdot 4H_2O$ were dissolved in 20 mL of deionized water and stirring for 30min. Then the solution was transferred to a Teflon autoclave for a hydrothermal reaction at 150 °C for 6 hours. The resulting $NiMoO_4$/NF were washed three times with deionized water and ethanol, respectively.

Preparation of $NiMoO_4@CeO_x$

The as-prepared $NiMoO_4$/NF was immersed in 0.1 M $Ce(NO_3)_3 \cdot 9H_2O$ for several seconds, then naturally dried in air for 10 min. Subsequently, it was immersed in 2.5 M NaOH for a few seconds, followed by natural drying for 10 min. Finally, the resulting $NiMoO_4@CeO_x$ was repeatedly washed three times with deionized water and anhydrous ethanol, respectively.

Preparation of CeO_x/NF

NF was immersed in 0.1 M $Ce(NO_3)_3 \cdot 9H_2O$ for several seconds, then naturally dried in air for 10 min. Subsequently, it was immersed in 2.5 M NaOH for a few seconds, followed by natural drying for 10 min. Finally, the resulting CeO_x/NF was repeatedly washed three times with deionized water and anhydrous ethanol, respectively.

Preparation of RuO_2/NF

5 mg of RuO_2 powder was mixed with 470 μL of ethanol and 30 μL (5 wt%) of Nafion solution by room temperature ultrasonication for 60 min to make the RuO_2 dispersed uniformly in the solvent. 100 μlink was loaded on 1×1 cm^2 pure nickel foam.

Characterization

The phase structure of the synthesized samples was characterized using an X-ray diffractometer (XRD: Rigaku SmartLab SE) The microstructure of the synthesized samples was characterized using scanning electron microscopy (SEM: GeminiSEM 500) and transmission electron microscopy (TEM: JEOL JEM-F200). The valence state and chemical components of the samples were carried out utilizing X-ray photoelectron spectroscopy (XPS: Thermo Scientific K-Alpha). The Raman spectroscopy was performed using a Renishaw in Via Qontor Raman system (523 nm).

Electrochemical measurements

The OER performance of the electrocatalysts were tested using a typical three-electrode mode on an electrochemical workstation (CHI 660E), with a Hg/HgO electrode and a platinum plate serving as the reference electrode and counter electrode, respectively. The Nernst equation is applied to convert potential *vs.* Hg/HgO electrode to potential *vs.* reversible hydrogen electrode (RHE):

$$E_{\mathrm{RHE}} = E_{\mathrm{Hg/HgO}} + 0.059 \times pH + 0.098$$

1.0 M KOH was used as respective electrolyte for OER. Linear sweep voltammetry (LSV) curves were recorded from 1.0 to 0 V (*vs.* Hg/HgO) at a scan rate of 5 mV s^{-1}. The electrochemical impedance spectroscopy (EIS) was performed in a frequency range of 100000–0.01 Hz.

Turnover frequency (TOF) number specifying the extent of evolved oxygen gas per unit of time was gained by electrochemical measurements. To calculate Ni loading of cataysts, successive CV scans were performed at different scan rates from 2.5 to 15 mV s^{-1} in the potential range covering the oxidation and reduction potential of Ni in 1.0M KOH. The obtained slope from the linear regression of the recorded oxidation current responses versus scan rate gives the mole number of Ni active sites:

$$\text{Slope} = \frac{n^2F^2A\Gamma}{4RT}$$

in which n refers to the number of electrons transferred during the oxidation of Ni^{2+} to Ni^{3+} (n=1), F is the Faradic constant, A is the geometrical area of the electrode (1 cm^2), Γ is moles per unit area for Ni active sites (mol cm^{-2}), R and T represent the universal gas constant and absolute temperature, respectively. m is the number of moles for Ni on the

surface participating in the OER and can be obtained by multiplying A by Γ: m=A×Γ. Afterwards, the TOF values based on Ni active sites were derived according to equation:

$$TOF = \frac{jA}{4Fm}$$

Where j is the current density (A cm^{-2}) of catalysts at a fixed overpotential, A is the surface area (1 cm^2), 4 indicates the four-electron transfer process in OER, F is the Faradic constant, and m presents Ni mole loading.

In situ infrared spectroscopy.

In situ infrared spectroscopy (Nicolet iS50) was employed to capture oxidation intermediates. The condition used for this test was same with Electrochemical measurements. The voltage was added from 1.1 V to 1.8 V (relative to the RHE). Spectral data were obtained by averaging 32 interferograms at 4 cm^{-1} resolution per potential step.

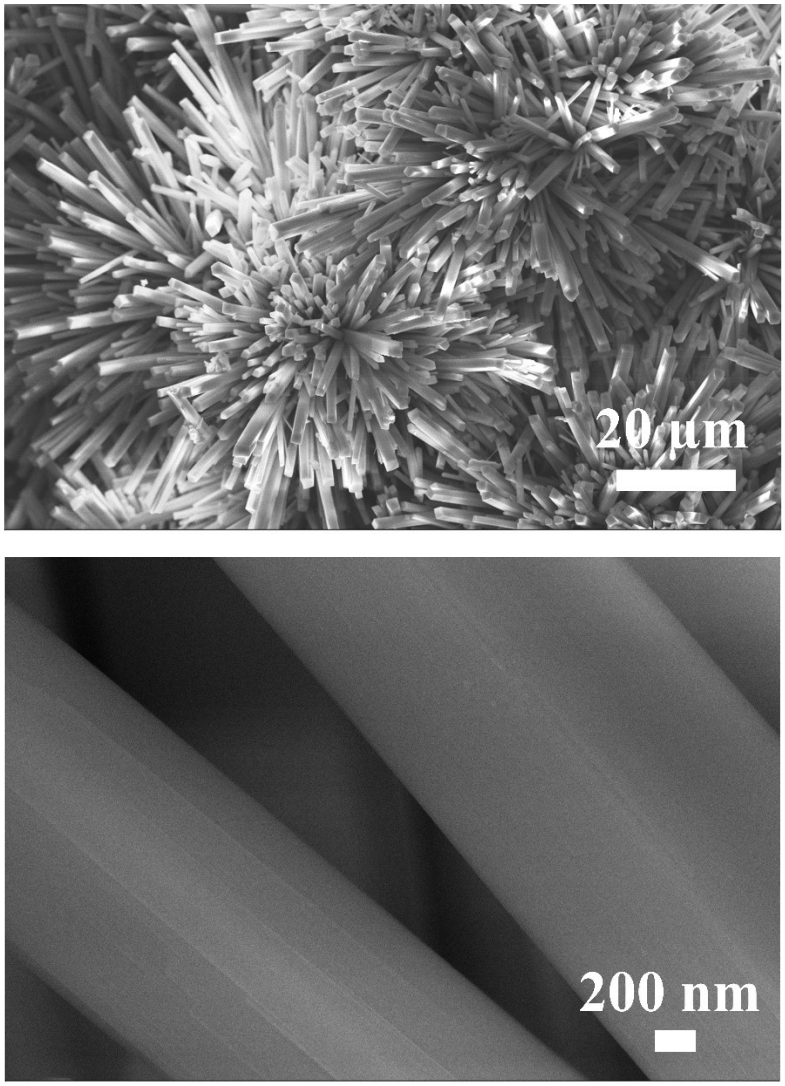

Fig. S1 SEM of $NiMoO_4$ (a-20 µm, b-200nm)

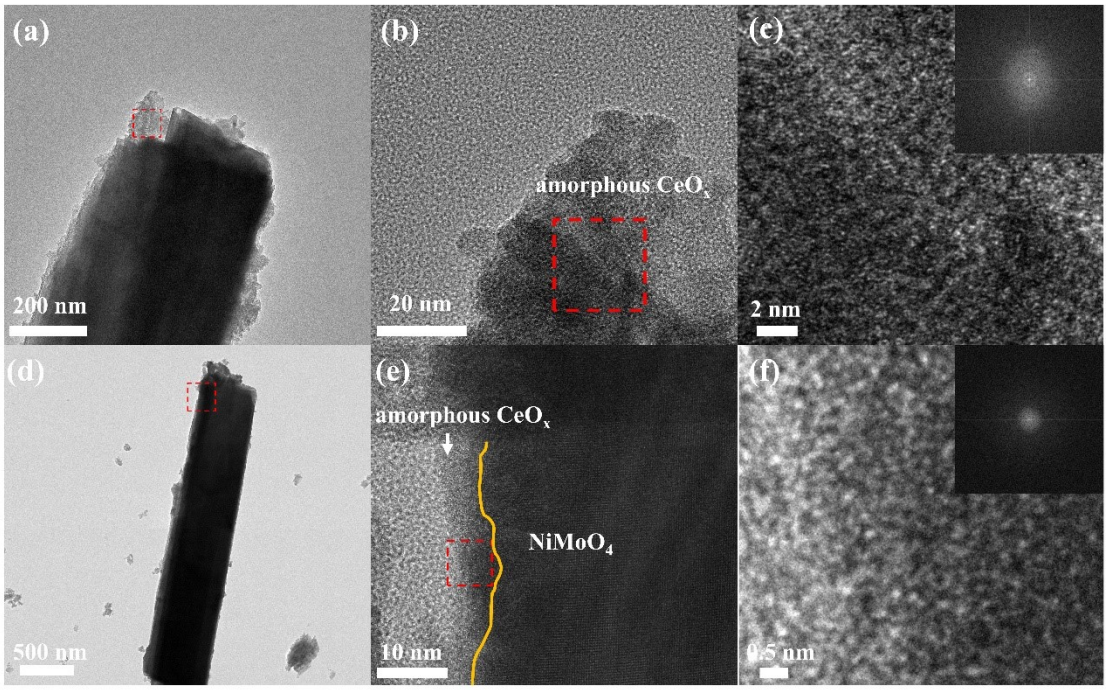

Fig. S2 (a), (d) TEM and (b), (c), (e), (f) HRTEM of $NiMoO_4$@CeO_x.

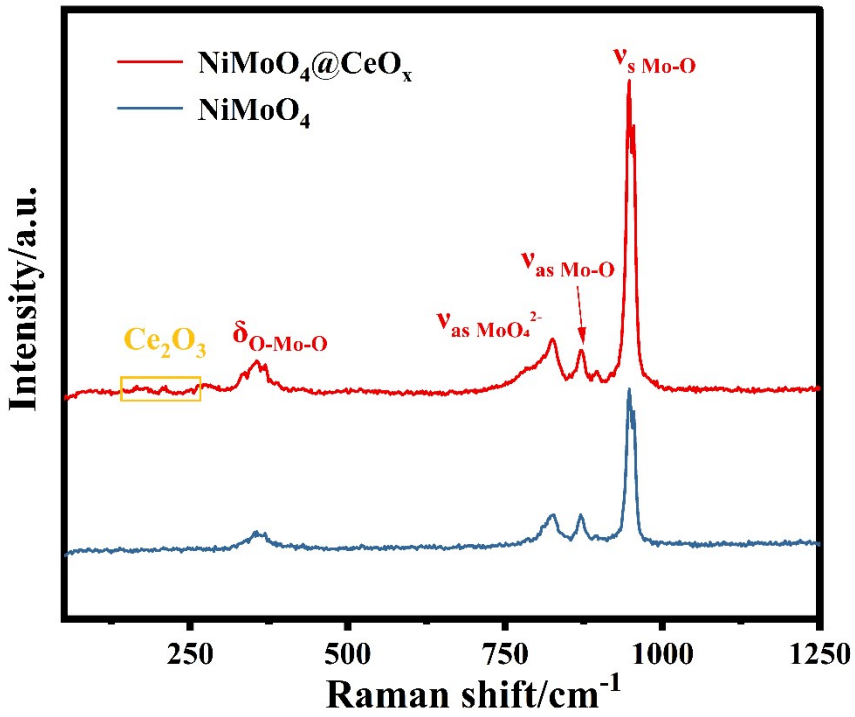

Fig. S3 Raman of $NiMoO_4@CeO_x$ and $NiMoO_4$

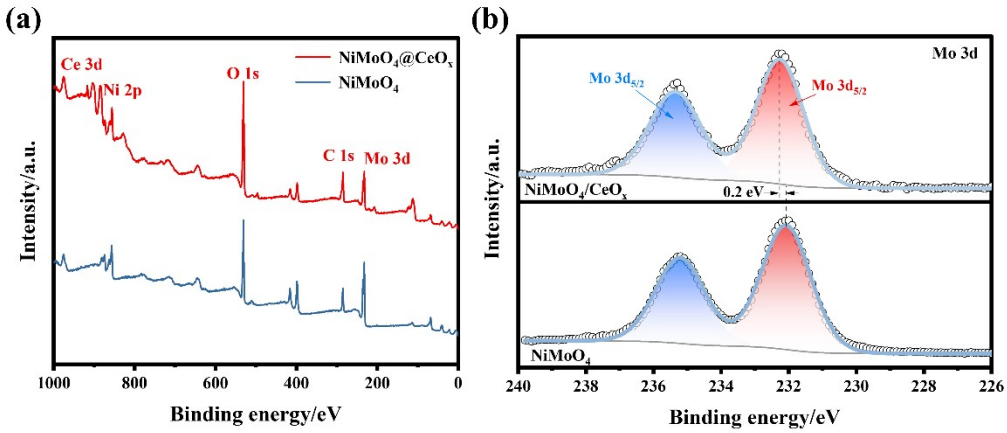

Fig. S4 (a)The full XPS spectra and (b) Mo 3d of $NiMoO_4$@CeO_x and $NiMoO_4$.

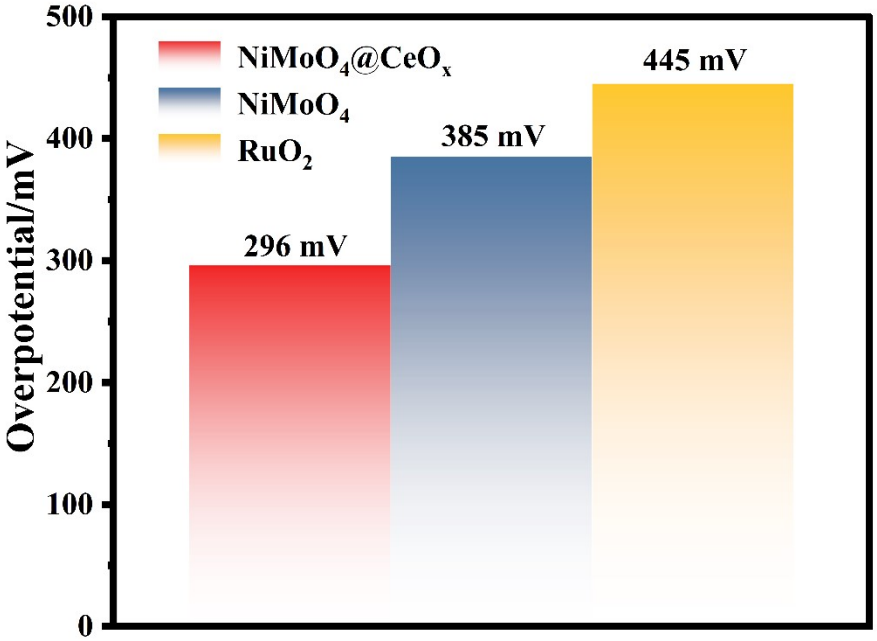

Fig. S5 Overpotential of $NiMoO_4@CeO_x$, $NiMoO_4$ and RuO_2 at 100 mA cm^{-2}.

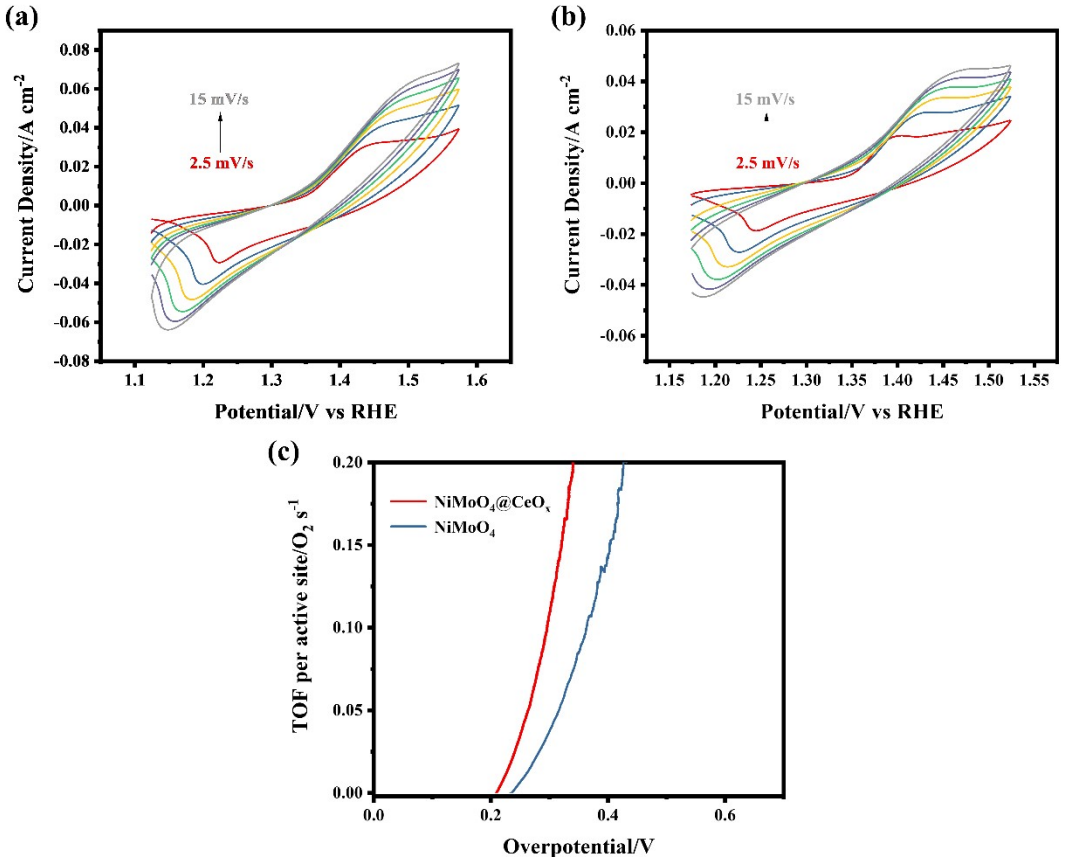

Fig. S6 CV curves at different scan rates for (a) $NiMoO_4$@CeO_x and (b) $NiMoO_4$. (c) Calculated O_2 TOF values.

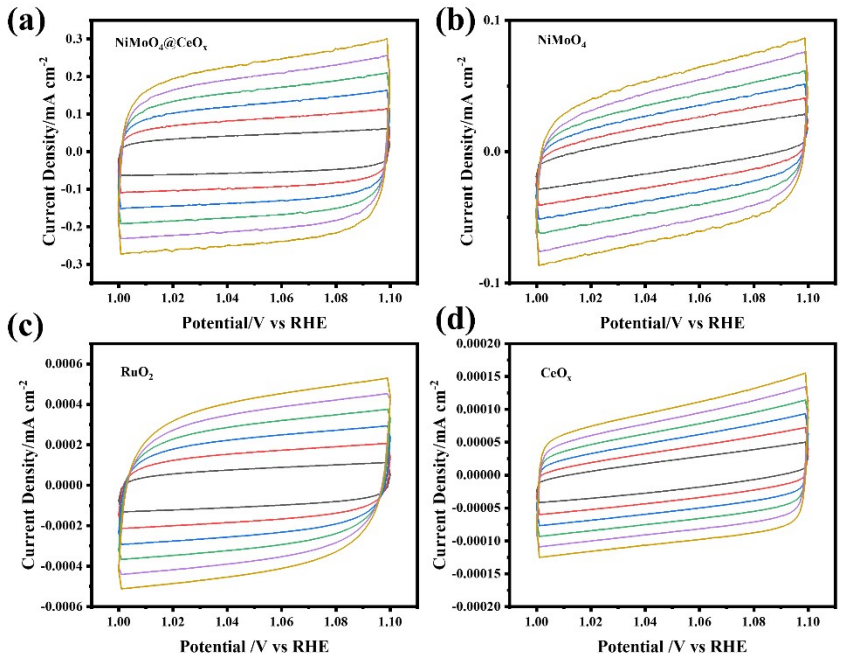

Fig. S7 CV curves of different scan rates of (a)$NiMoO_4$@CeO_x, (b)$NiMoO_4$, (c)RuO_2 and (d)CeO_2.

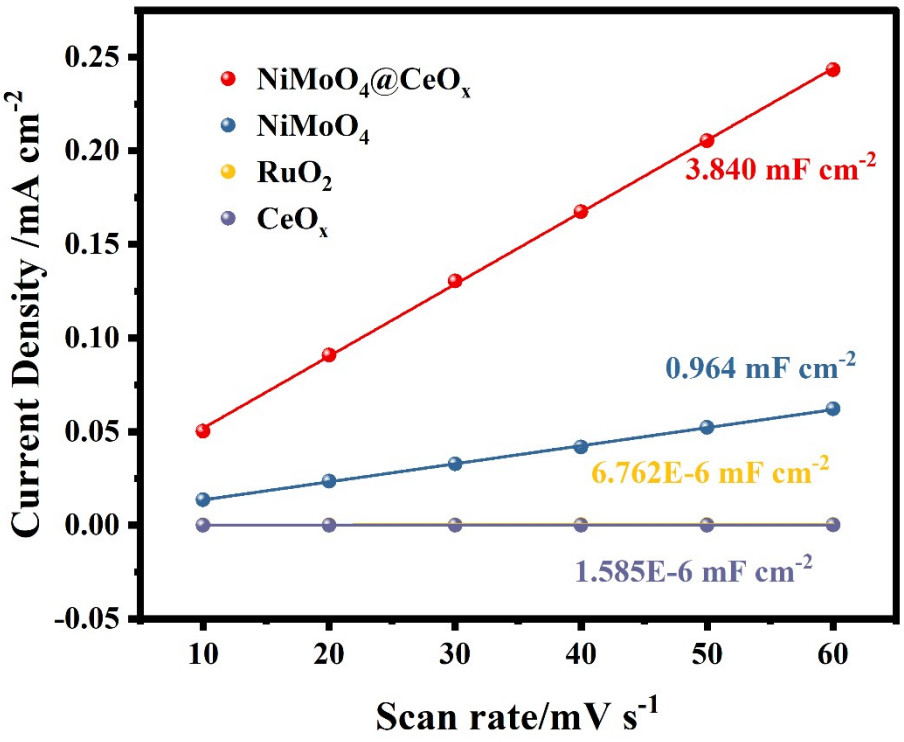

Fig. S8 C_{dl} plot of ctatlysts.

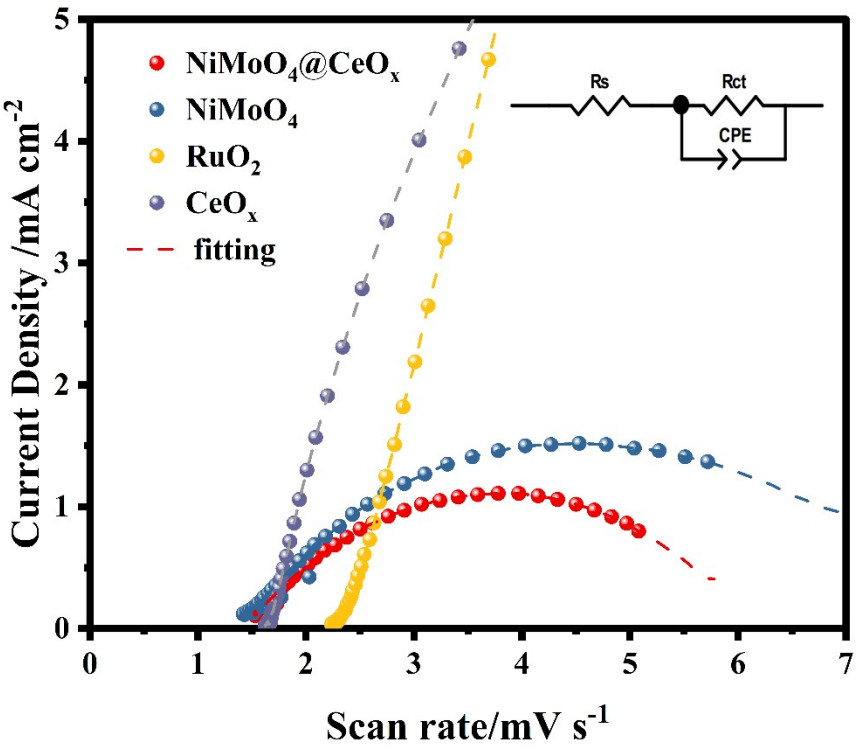

Fig. S9 The Nyquist plots of catalysts.

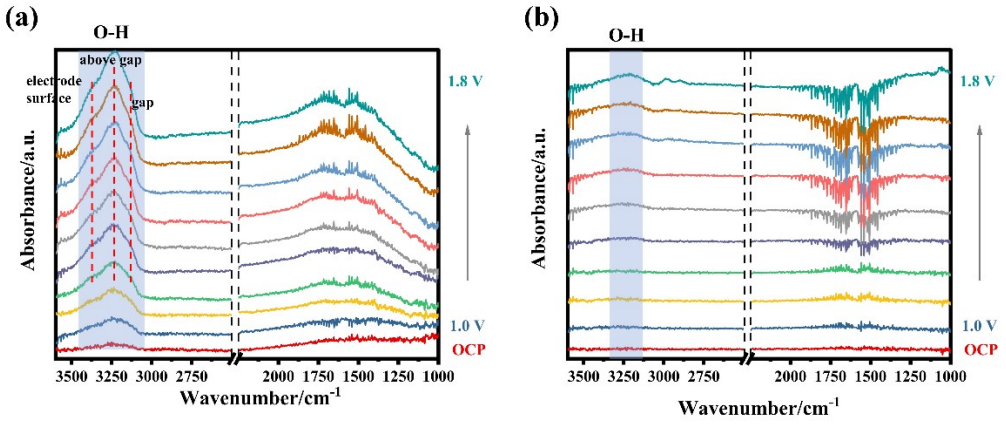

Fig. S10 In situ FTIR spectroscopy of (a) $NiMoO_4$@CeO_x and (b) $NiMoO_4$.

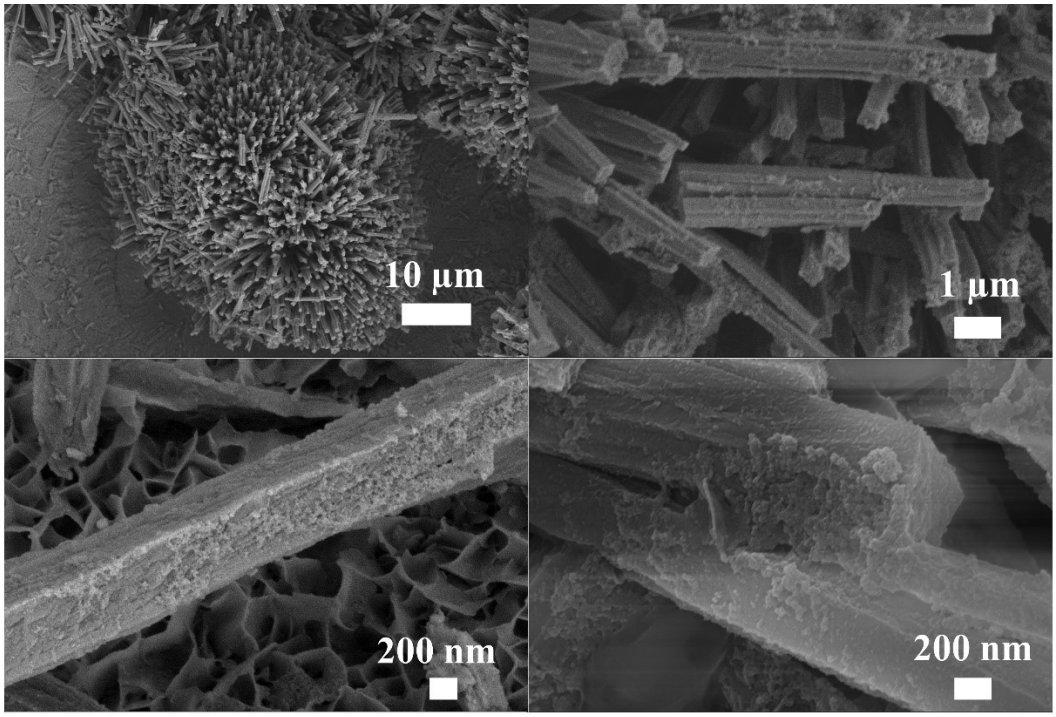

Fig. S11 SEM of $NiMoO_4$@CeO_x after stability.

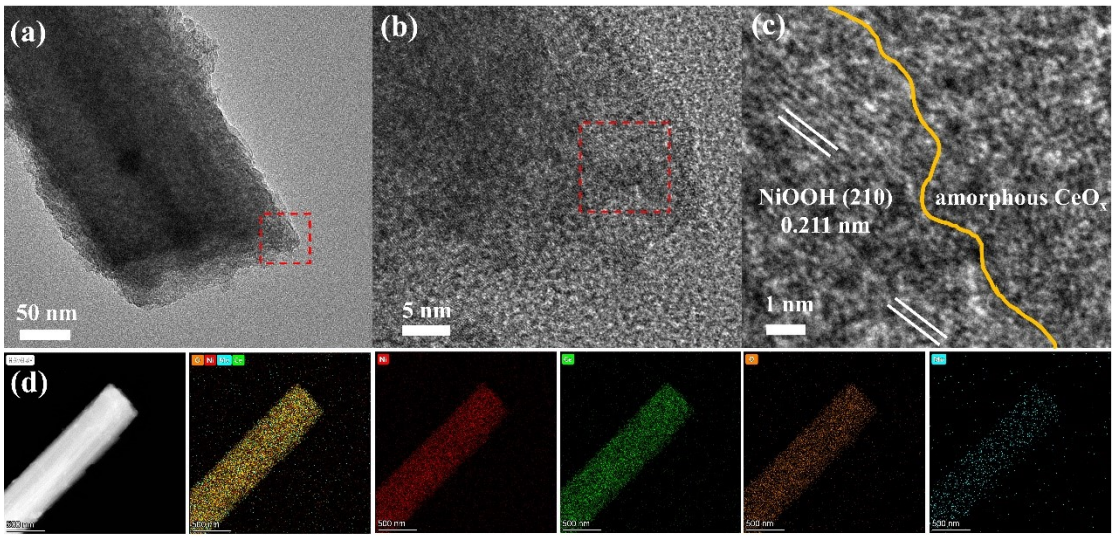

Fig. S12 (a) TEM, (b-c) HRTEM, and (d) HAADF-STEM of $NiMoO_4$@CeO_x after stability.

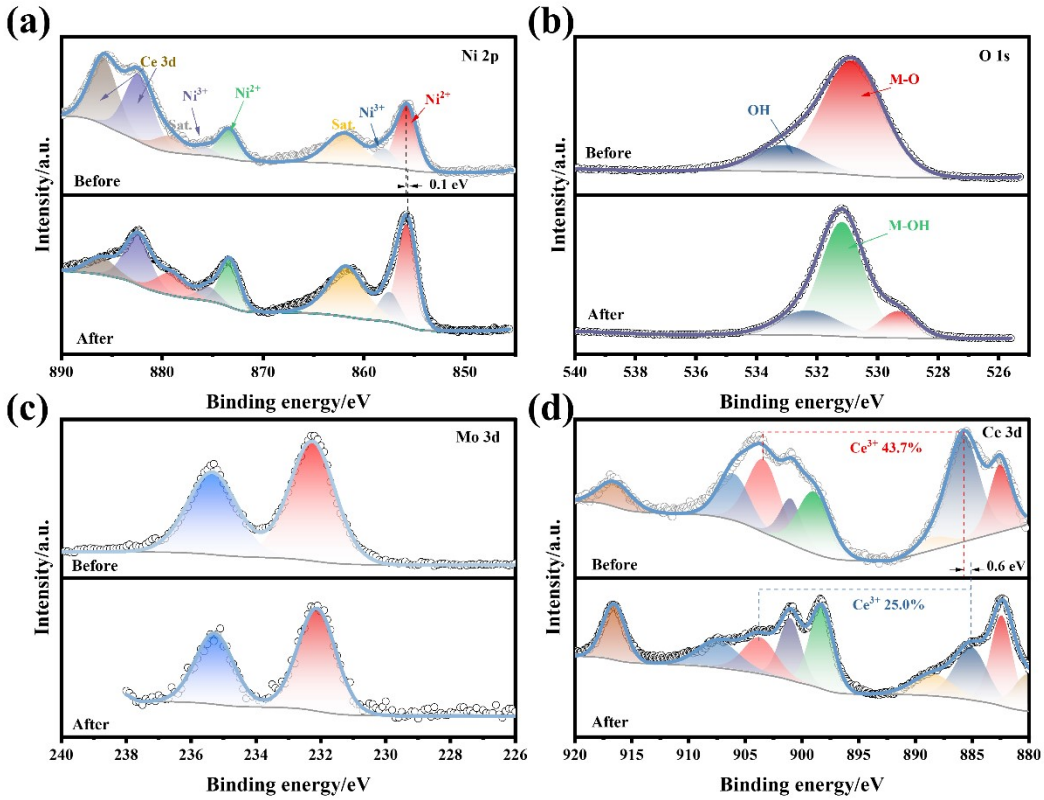

Fig. S13 XPS before and after stability test of $NiMoO_4$@CeO_x

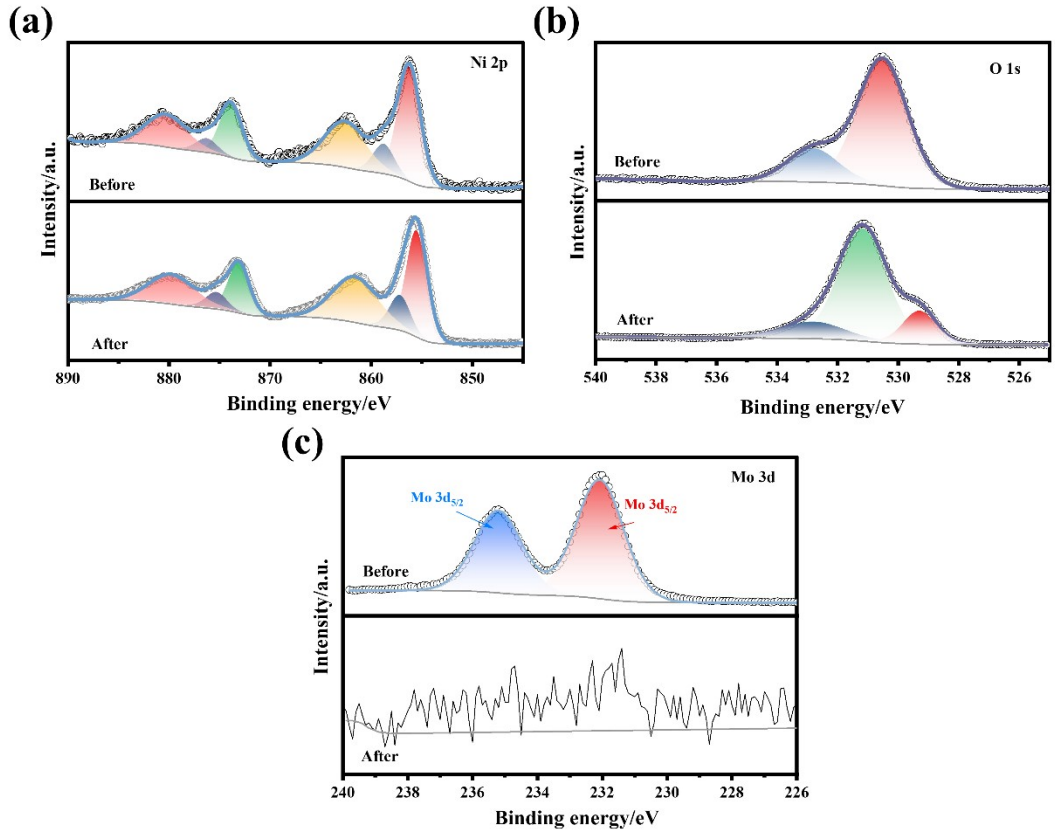

Fig. S14 XPS before and after stability test of $NiMoO_4$.

Table S1. The ICP-OES data for $NiMoO_4@CeO_x$.

Catalyst	**Ni (wt%)**	**Mo (wt%)**	**Ce (wt%)**
$NiMoO_4@CeO_x$	29.57	36.75	2.65